Polarization-fluorescence Microscopy in the Study of Aggregates and Concrete

Maarten A.T.M. Broekmans[1], Isabel Fernandes[2], Ola Fredin[3], and Annina Margreth[1]

Fluorescence micrograph of intensely weathered biotite in saprolite from western Norway. PHOTO: ANNINA MARGRETH.

1811-5209/22/0018-0321$2.50 DOI: 10.2138/gselements.18.5.321

Concrete structures may develop deleterious damage, which significantly reduces service life, structural integrity, and safety, posing serious issues in large or otherwise critical infrastructure. Routine petrographic assessments, including microstructure, texture, and fabric, of concrete and its (gravel and sand) aggregate and binder constituents in thin section using polarization-fluorescence microscopy (PFM) enables the unequivocal identification of features that would otherwise remain hidden in conventional petrography. Rigorous preparation procedures preserve original microstructural details, make preparation artefacts recognizable, and ensure that the fluorescent emission can be quantified. This contribution outlines the preparation of fluorescence-impregnated thin sections and elaborates on the application of PFM to damaged concrete, with further examples from selected rock types commonly used for concrete aggregate.

KEYWORDS: polarization-fluorescence microscopy (PFM); thin section preparation; microporosity; microcrack fabric; concrete damage; unconsolidated natural rocks

INTRODUCTION

Concrete structures exist by virtue of their combined material (coarse aggregate, fine aggregate, and binder) and structural (beams, arches, girders, reinforcement, and prestressing) properties (Gordon 1978). The default 'traditional engineering method' for assessment of 'concrete quality' during the construction of structures above a certain size is based on compressive strength testing. This is traditionally performed on cubes produced from the actual job mix cured at room temperature immersed in water for 28 days, yielding the so-called 'norm-strength' in megapascals (MPa). Common additional test methods include tensile strength, density, water ingress depth from the surface (splitting a cube after one-sided exposure, in mm), total porosity (gravimetric, water-saturated cube minus dry cube weight, in vol%), but many more are available (e.g., ASTM 2022).

With some modifications, the above tests may also be applied to core samples drilled from existing structures if the concrete is suspected to be underperforming or is visibly degrading, leading to a reduction of the projected service life, intended functionality, and/or user safety. Testing of bulk concrete is highly relevant to the practical aspects of a structure in service, such as load-bearing capacity and infiltration of de-icing salts or seawater (potentially causing reinforcement corrosion). However, any local property variations at the sub-cube (core) scale remain undetected and are further smoothed out in a calculated average. Just as a field geologist must consider the representativity of a backpack full of rock samples for an entire granite aggregate quarry (and the tiny fraction that actually lands under the microscope in a thin section), a concrete petrographer must consider how observations on thin sections scale to the structure as a whole (Broekmans and Fernandes 2015).

Concrete decay processes include dissolution and precipitation of phases, chemical reactions between solid and fluid phases (e.g., water, carbon dioxide, aggressive media), as well as physical processes such as abrasion, stress deformation under load, thermal expansion, and freeze/thaw cycling (i.e., expansion of water freezing in micropores), etc. Some of these processes are known from the weathering, alteration, reactive transport, and erosion of natural rocks, while some are unique to concrete (e.g., Poole and Sims 2016). Most often, chemical and physical decay processes work in concert, making it a challenge to distinguish cause from consequence.

By far, the majority of decay cases are fluid-mediated whether via infiltration, dissolution, transport, leaching, or escape (during fire). In sound concrete, fluid housekeeping is dominated by diffusion through the intrinsic porosity of the hydraulic binder (typically ~15 vol%). The presence of 'imperfections' in concrete, whether construction flaws from poor workmanship or design, or the introduction of fissures, dramatically enhances local fluid flow and access, converting an initially 'closed concrete system' into an open system. Therefore, porosity, permeability, and their spatial distribution are crucial parameters in the assessment of concrete decay mechanisms. Correct identification of the cause(s) is essential to determine a diagnosis and/or effective repair strategy, or to justify demolition, or alternatively, warranty claims and legal liability in newer structures.

1 Geological Survey of Norway – NGU
PO Box 6315 Torgarden
N-7491 Trondheim, Norway
E-mail: Maarten.Broekmans@ngu.no
E-mail: annina.margreth@ngu.no

2 University of Lisbon
Faculty of Sciences
Department of Geosciences & Instituto Dom Luiz – IDL
Campo Grande Edifício C1-Piso 1
1749-016 Lisboa, Portugal
E-mail: mifernandes@ciencias.ulisboa.pt

3 Norwegian University of Science and Technology – NTNU
Department of Geoscience and Petroleum
PO Box 8900 Torgarden
N-7491 Trondheim, Norway
E-mail: ola.fredin@ntnu.no

Petrographic assessment starts with planning a sampling campaign well ahead of time, concrete being no different from natural rock samples in this respect. Rigorous application of cautious sample extraction and handling procedures from field to laboratory minimizes the attribution of (micro)structural and/or compositional artefacts (Broekmans 2012).

In field geology, optical thin section petrography is the go-to method to determine further analytical strategies for newly collected samples. In civil and concrete engineering, however, petrography is too commonly seen as the last-resort method when results from traditional testing remain inconclusive (Broekmans 2009; Fernandes et al. 2009), despite the wide availability of (inter)national standards and guidelines elaborating the procedures to follow (Poole and Sims 2016; Sims and Poole 2017 and references therein). This lack of popularity may at least in part be due to petrographic observations not being reported as simple numbers, but as written text requiring relevant competence.

Polarization-fluorescence microscopy (PFM) is a powerful and cost-effective method for 'quality assessment and control' (QA/QC) throughout the life of structural concrete, from verifying the content of potentially deleterious (silica) minerals in virgin aggregate prior to actual use (Fernandes et al. 2016) and QA/QC of the 'as delivered' concrete in a structure (e.g., homogeneity, degree of compaction) to the assessment of concrete degradation when observed in a structure and suitability of recycled concrete for reuse as aggregate.

This paper outlines the procedures for preparing thin sections to assess damaged concrete using PFM, and its application to damaged concrete and selected rock types of natural origin. Existing routines for ordinary thin section preparation are modified to visualize internal microporosity and/or cracks, requiring minimal investment in supplementary equipment and instrumentation, and to avoid preparation artifacts. The same preparation routines can be used to visualize microstructural and textural features in deformed, weathered, unconsolidated rocks, sediments, or other rock types, that otherwise remain hidden with default routines (Camuti and McGuire 1999). This method presents a dramatic contrast improvement compared to the use of blue epoxy (cf. Yanguas and Dravis 1985), as we will show with examples.

MATERIALS AND METHODS

Preparation of Fluorescence-impregnated Thin Sections

The pore network in hydrated cement paste is formed during construction when water is added to the concrete mix, and growing prisms and platelets of clinker hydrates touch to form an intricate three-dimensional nanoscale network, its density being affected by the amount of excess water present (i.e., not bonded in hydrates). The overall pore volume in cement paste may be as large as 15–20 vol%, initially reflecting the water–cement ratio used, but evolving further upon aging. In contrast, the internal porosity of an aggregate particle mainly consists of the interstitial space along mineral grain boundaries in supracrustal rock types, and cracks in deformed rocks, and is generally 2–3 orders of magnitude lower than in the paste (exceptions being chert/flint and opaline limestone).

Furthermore, the clinker hydrates composing the bulk cement paste in ordinary Portland cement (OPC) concrete form foils, platelets, and fibers only a few tens of nanometers thick (Odler 1998). They are also mechanically soft, with Mohs scratch hardnesses of ~3 and below. Without a sturdy 'scaffolding', the fragile paste crystallites break or bend rather than being cut off by the abrasive during cutting to size, lapping to thickness, and polishing to finish. Moreover, fine and mechanically rigid particles (e.g., aggregate quartz, unhydrated clinker relics) may get dislodged from their bedding (aka 'plucking'), acting as additional 'stray abrasive' milling down softer parts in an uncontrollable manner. Both debris and abrasive particles get relocated and deposited in pores, a contamination artefact in some thin sections. To petrographically identify very fine-grained constituents (e.g., relic clinker, blast furnace slag, fly ash particles), concrete sections must be thinned to ~15–20 µm, rather than the default 30 µm in typical geological practice, to minimize overlaying grains. Therefore, default thin section preparation procedures must be extended with a few additional steps to ensure that delicate sample materials, such as damaged concrete (or any other fragile/porous sample material), survive the abrasive process.

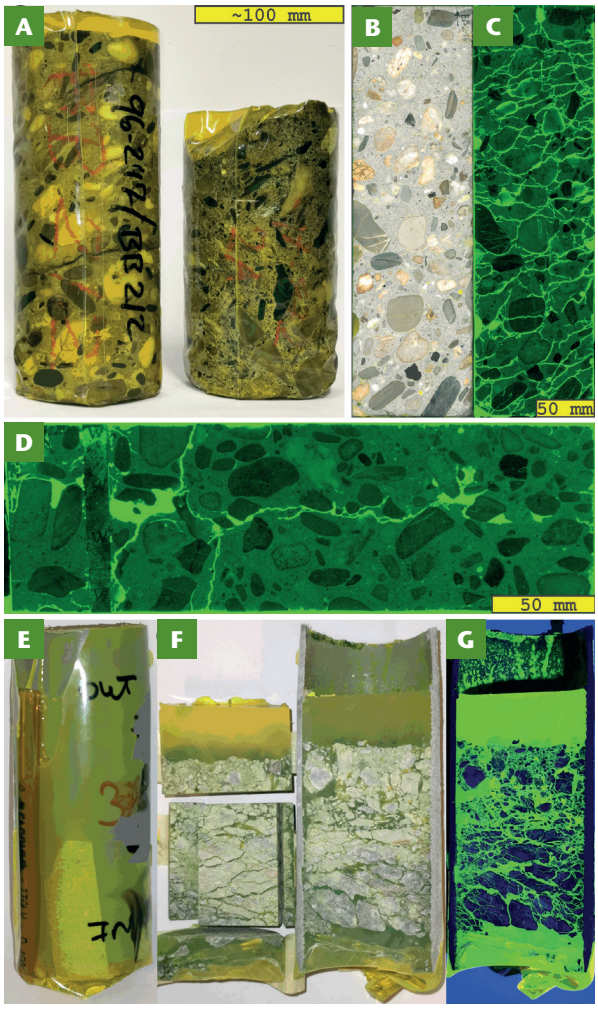

Figure 1 (**A**) Two impregnated full cores (**left** Ø100 mm, **right** Ø110 mm). The flat structure surfaces are at the bottom so the cores stand upright unsupported during impregnation. (**B**) A fully impregnated Ø100 × 400 mm drill core from an alkali–silica reaction (ASR)-damaged structure reveals no cracking in plain light (orientation as in the structure). (**C**) The same core in fluorescence reveals pervasive local cracking that crosses coarse aggregate particles. (**D**) In reality, the horizontal 'crack' is the contact between two concrete batches poured on different days. A vertical reinforcement bar (orientation as in the structure) is visible at left. (**E**) The 'Kubiëna box' core from the fault gouge in Figure 3A, with part of the plastic hose for impregnation still visible to the left. (**F**) The same core sliced lengthwise and flipped, thin section billet extracted from the approximate center. (**G**) The right core half in fluorescent light from a 'bargain basement'–priced 21 LED 'UV-torch', photographed with a cell phone.

A preparation protocol was first outlined by Wilk et al. (1974) with an elaboration on its application and use by Romer and Dobrolubov (1974). A practical step-by-step laboratory protocol with a list of materials is outlined in the Dutch national guideline, CUR-Recommendation 102 (2008), and a generic background is given in Ingham (2011) and Poole and Sims (2016).

Under ambient conditions in a moderate climate at 75% relative humidity, pores finer than ~1.0 µm are filled with molecular water from surface absorption combined with capillary condensation (Hens 2012). Occupied pores obstruct access to connected larger pores ('bottlenecking'), which effectively inhibits the penetration of fluid epoxy. Therefore, sample portions for thin sectioning are dried prior to impregnation. Temperatures must not exceed ~50 °C as some hydrated phases in concrete (e.g., ettringite) decompose and/or decrepitate, causing shrinkage cracking as an artefact at higher temperatures. The pre-dried sample portions are then transferred to a (low) vacuum chamber while hot and pumped down to ~1 mPa. This removes most remaining water, making the pore network accessible for epoxy impregnation (pressurized impregnation does not have this drying effect).

A vacuum impregnation apparatus (modified after Ashley (1973)) consists of a suitably thick polycarbonate tube chamber Ø300 mm/12″ on an aluminum base and covered by an aluminum lid with a valved connector for a vacuum hose, and additional transits for disposable plastic tubing Ø6 mm/0.25″ with a simple clamp valve to admit freshly mixed epoxy from the outside. Grooved slots with O-rings in the metal base and lid ensure air tightness. The chamber is vented when all samples are fully immersed in the liquid epoxy; the atmospheric pressure then further pushes in the still-liquid epoxy. Depending on the overall height of the polycarbonate chamber, (pre-dried) drill cores can also be impregnated by tightly wrapping them in polyethylene bags with the plastic tubing reaching down to the bottom of the sample (Fig. 1). Immediately after venting, the bags with fully epoxy-immersed cores must be transferred to pails with cold water to prevent the strongly exothermic epoxy-setting reaction from creating vapor bubbles.

Epoxy and Fluorescent Dye

'Epoxy' is a generic term for a class of two-component (i.e., resin, hardener) thermosetting organic polymers, available with a broad range of physical properties in the liquid state, as well as when fully cured. A particular combination of properties is required for the effective impregnation of porous aggregates and concrete for thin sectioning. Low viscosity and good surface-wetting capability ensure that the liquid epoxy readily enters the finest pores and interstices by capillary suction (as opposed to, for example, liquid mercury used in microporosity testing), whereas a low volatile content prevents the freshly mixed liquid from boiling up excessively under vacuum.

Further requirements include low curing shrinkage, good adhesion and rigidity (Shore hardness and bulk modulus) to offer mechanical support during lapping and resistance against the implantation of debris during preparation, and a suitable refractive index near that of quartz, as well as no discoloration, shrinkage, crystallization, or debonding upon normal use and aging (e.g., Jägers et al. 2000).

For in situ analysis (e.g., scanning electron microscope/energy dispersive X-ray spectrometry (SEM/EDS), electron probe microanalysis, laser ablation inductively coupled plasma mass spectrometry, secondary ion mass spectrometry), it is important to know that epoxy contains elements in detectable amounts other than the nominal organic species, and various additional species have been identified in different products (The University of Edinburgh 2022).

Many thin section laboratories use a dye known as Fluorescent Brilliant Yellow R (CAS Common Chemistry 2022), which is readily available at low cost from many suppliers under many different names. A tried and tested recipe for preparing fluorescent epoxy is given in the Dutch national guideline CUR-Recommendation 102 (2008). The dye must be completely dissolved in the resin without bottom residue (using a magnetic stirrer) before adding the curing compound. If the dyed epoxy is similar to the color of the mineral constituents in ordinary plane-polarized light (e.g., thaumasite, palagonite), then an alternative dye with a more contrasting color can be chosen.

The Brilliant Yellow dye uses blue light from standard halogen or LED microscope illumination for excitation (optimum at 485 nm, i.e., blue light) to luminesce in a bright greenish yellow (emission at 545 nm). Contrary to popular belief and even some published sources, specialized high-intensity ultraviolet (UV)-light sources are not necessary, which saves on instrumentation cost, reduces photo-bleaching of the dye upon exposure to 'hard UV', and is safer for the petrographer's occupational health.

The optical microscope is (retro)fitted with an excitation filter to admit only blue light to the specimen, and an emission filter to permit only the fluorescence to reach the petrographer's eye. Optimum luminescence is achieved in incident illumination where each objective is its own condenser, but fluorescence in transmitted light is fully functional. Quantification of the luminescence is accomplished using a photocell (as for the reflectance of ore minerals), which integrates over the viewing area, or in a more sophisticated manner, using a digital camera and image processing (e.g., Elsen et al. 1995; Wong et al. 2020). The color variation in the thin section micrographs further down in this paper is due to the use of different digital cameras or (negative or slide) films.

In structural concrete, the crack fabric is crucial to help distinguish the primary cause of deterioration (notably, internal expansive reactions and frost damage, but also sampling artefacts from core drilling) by fluorescence-assessment of impregnated full cores, as mentioned above. After the epoxy is fully set, the cores are cut lengthwise to reveal the internal crack pattern using a simple purple (often wrongly dubbed 'UV') LED torch (Fig. 1C and 1D). Filters are not necessary, neither for direct observation of the impregnated full cores nor for photography (Fig. 1G). Detailed assessment of the impregnated core using a stereo microscope in plain and fluorescent illumination is helpful to select areas for subsequent thin sectioning after reiterated impregnation of cut portions (Broekmans 2012).

EXAMPLES AND DISCUSSION

Characterization of Aggregates for Concrete

While PFM was originally introduced for detailed quality assurance/control of (damaged) concrete, it can/should also be applied to assess the microstructure and microtexture of virtually *any* geological material regardless of origin. Some illustrative examples are elaborated below.

Petrography of soils (aka 'micropedology') was pioneered by Kubiëna (1938) and involves the in situ assessment of mineral content, particle morphology, porosity, permeability, and sedimentary microstructure and microtexture (e.g., Camuti and MacGuire 1999). In current practice, the assessment of unconsolidated sediments, glacial deposits, soils, and deeply weathered bedrock typically includes on-site field descriptions and grain-size distribution analysis of bulk material in the laboratory. The RILEM AAR-1.1 test method (RILEM 2016) specifies minimum sizes for representative samples of coarse (gravel) and fine (sand) aggregate for use in concrete. Polarization-fluorescence microscopy reveals the internal microstructure of aggregate

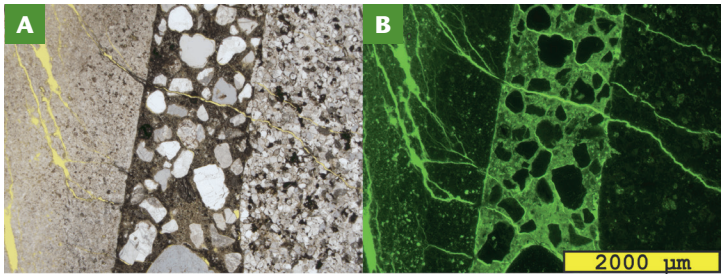

Figure 2 Internal porosity and partial dissolution from deleterious ASR in Dutch chert particle in (**A**) plane-polarized light and (**B**) polarization-fluorescence microscopy (PFM). The results in (**B**) reveal the presence of many more fine cracks that, in plane-polarized light, remain inconspicuous, even when the epoxy is dyed yellow. Moreover, lithic fragments and altered K-feldspars in the sandstone particle light up in (**B**).

materials in much greater detail than conventional plane- or cross-polarized light, enabling precise in situ identification of precursor minerals to the weathered product, and the effects of mineral alteration on the microstructure and microtexture (Fig. 2).

According to applicable standards (e.g., ASTM D75M-19 (ASTM 2022); RILEM AAR-1.1 (RILEM 2016)), modal contents in volume percent of all lithologies present in virgin aggregate >4 mm (gravel) are determined by visual assessment and separated by handpicking. The fractions are then weighed to determine the relative proportions of all particles from a sample mass considered representative of the standard. However, the mineral (modal) content, microstructure, microtexture/microfabric, and internal porosity that affect the aggregate performance with respect to the deleterious alkali–silica reaction (ASR) remain essentially unassessed, even more so for fine size fractions <4 mm (sand). Therefore, to prevent deleterious ASR, all size fractions are nowadays assessed by PFM prior to use in a concrete mix (see Broekmans 2012; Fernandes et al. 2016).

Intra-deposit variation is a well-known phenomenon in metals mining, and the extraction industry makes a lot of effort to 'avoid the bad parts'. There is no reason why construction aggregate deposits would be exempt to such natural variation, notably regarding the ASR potential. Rocks with a tectonically deformed microstructure (e.g., mylonite with undulatory quartz, cataclasite, fault gouges) are typically more prone to deleterious ASR than their non-deformed counterparts.

Polarization-fluorescence microscopy has proven instrumental in revealing additional microtextural detail of the rock precursor and the identification of primary, protolithic minerals transforming into secondary, authigenic minerals arranged in a neogenic fabric. For example, quartz grain boundaries in sandstones subject to compaction and cementation by diagenetic dissolution/precipitation are difficult to identify using conventional petrography but are readily distinguished by PFM.

Another example of the relevance of PFM for geological applications is found in the Goddo Fault (Norway). This fault zone is characterized by a large, smooth, gently undulating, principal slip surface, which is overlain by an approximately 0.5–1 m thick layer of immature, indurated cataclasite (Fig. 3A). The cataclastic fault core can be further subdivided into two distinct and spatially separated structural domains: a ~0.3 m thick greenish layer of fine-grained gouge immediately overlaying the principal slip surface; and a grey-reddish, gently undulating phyllonite with a clearly visible fish-scale fabric. The gouge was sampled by hammering a Ø45 mm plastic tube into the outcrop (Fig. 3A) as a type of Kubiëna box. After controlled drying, the tube was impregnated with fluorescent epoxy (as in Fig. 1G), sliced lengthwise when fully set, and a polished section was prepared from the core interior (see Fig. 1F) to exclude potentially deformed sample edges (Viola et al. 2016).

The polished section prepared from the fault gouge provides essential details for the interpretation of the complex deformation history. Observation in ordinary plane (Fig. 3C) and cross (Fig. 3D) polarized light reveals coarse clasts floating in a fine-grained ground mass of sericite and clay minerals with embedded clasts of individual quartz or feldspar grains. Coarse clasts may consist of mylonite with sub-graining, undulous extinction, and shear banding as visible along the upper edge of the main particle (Fig. 3D), or cataclasite, deformed K-feldspar grains, or quartzite containing minor carbonate.

Fluorescent illumination (Fig. 3B) reveals the presence of a dense fracture network detaching the clast from the surrounding matrix, but also locally cross-cutting clasts and partly filled with detritus toward the clast interior.

In Norway, the alkali-reactivity potential of cataclasite has been tested using laboratory expansion tests over the last decades (Lindgård et al. 2010). More recently, cataclastic material was tested to determine the release of alkalis in concrete (Menéndez et al. 2022). Petrographic assessment of this rock is quite challenging because of its intense deformation and fine mineral grain size, and element mapping by SEM/EDS has proven useful to determine mineral (modal) contents. Detailed petrographic analysis of ASR-damaged concretes containing cataclasite particles classified the rock type as potentially alkali-reactive (Class II in RILEM AAR-1.1 (RILEM 2016)), confirming experience from field structures and expansion testing.

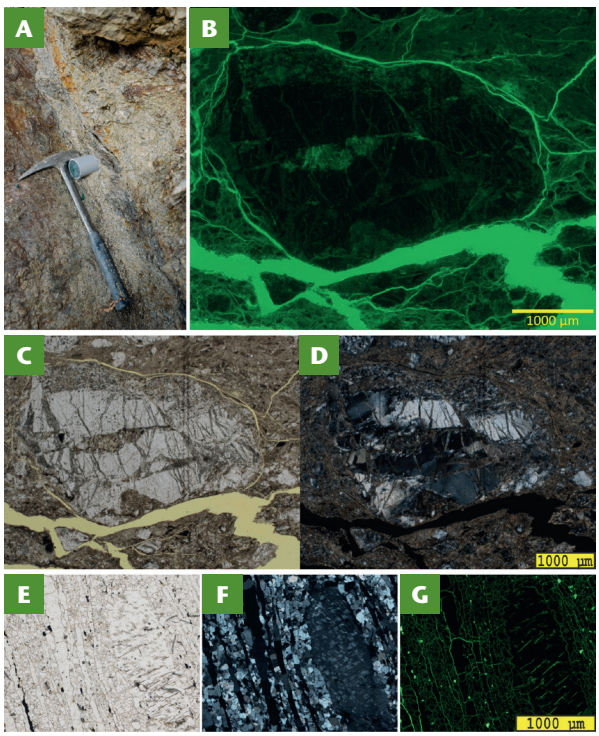

Figure 3 (**A**) Kubiëna-type sampling of greenish clay-rich gouge lying between the principal slip surface (the reddish surface on which the hammer is resting) and the grayish red phyllonite, using 40-mm-wide PVC (polyvinyl chloride) drainage tubing (also see Fig. 1E–1G). Micrograph of a mylonite clast floating in a fine-grained clastic ground mass in (**B**) fluorescence, (**C**) plane-polarized, and (**D**) cross-polarized light. (**E**) Blastomylonite with characteristic ribbon quartz running north-northeast–south-southwest, (**F**) appearing near-black in cross-polarized light, and patchy K-feldspar, the latter of which shows internal cracking in (**G**) fluorescence.

Application to the Study of Concrete

Petrography of hardened concrete has a long history (e.g., Mather 1953 and references therein), mainly for the diagnosis of deterioration but also to obtain the composition of concrete mix designs in cases where this information is missing.

Polarization-fluorescence microscopy is gradually being recognized as one of the better methods for the determination of the water/cement (w/c) ratio in hardened concrete. Recently, Wong et al. (2020) published results from the largest Round-Robin test yet held to determine the method's accuracy. Polarization-fluorescence microscopy was convincingly shown to provide accurate estimates of the w/c ratio in concrete mixes, even better than the default physico-chemical method. Figure 4 presents examples of a set of thin sections used in the study.

In addition to determining the w/c ratio, PFM is arguably most commonly applied to diagnose concrete deterioration. The potential causes for cracks in structural concrete are many, but among the most feared is deleterious ASR, in which silica in the aggregate (i.e., opal, chalcedony, quartz, silica polymorphs) enters into a reaction with alkalis (i.e., Na, K) dissolved in the pore water, forming a reaction product that attracts and reacts with water (i.e., both hygroscopic and hydraulic), thereby expanding and fracturing the surrounding concrete (Broekmans 2012; Sims and Poole 2017 and references therein) (Figs. 5, 6A, and 6B). The initially amorphous and glassy ASR reaction product ('gel') often crystallizes upon aging, which is then referred to as 'ASR reaction product' (Leemann et al. 2016).

In addition to ASR, and in some cases occurring concurrently, delayed ettringite formation (DEF) is an internal reaction that is easily detected under optical microscope because of the characteristic texture/fabric of ettringite deposits. Delayed ettringite formation occurs if the internal temperature of the concrete mix rises above 65 °C immediately after pouring (e.g., Odler 1998), above which deleterious clinker-hydration reactions become predominant. The resulting crack pattern is distinct from ASR, and PFM constitutes the most reliable method to distinguish these deterioration mechanisms, ahead of considerably more expensive SEM/EDS analyses of crack-filling deposits.

In sewer systems, concrete deterioration may appear dramatic with strong delamination of the concrete, usually at very low pH and resulting in new products (Fig. 6C and 6D). Again, in this case, PFM is the preferred method to visualize the disturbed microtexture of the concrete and the porosity increment of the aggregate particles.

In addition to internal expansive reactions, the study of rocks and concrete affected by fire can benefit from the use of PFM. Fire effects on concrete are observed in hand samples by regions of reddish discoloration that crumble readily and must be handled with extra care, but

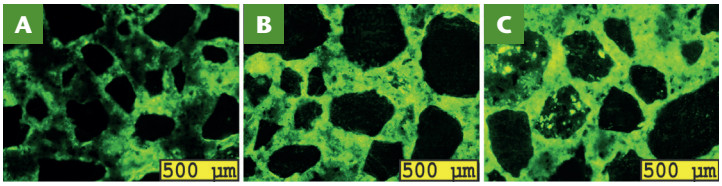

Figure 4 Increasing intensity of fluorescence, reflecting that the internal porosity in cement paste is related to increasing water/binder ratio, from 0.35 (**left**) to 0.50 (**right**), as used in the RoundRobin test (Wong et al. 2020). Thin sections courtesy of RSK Environment Ltd, United Kingdom.

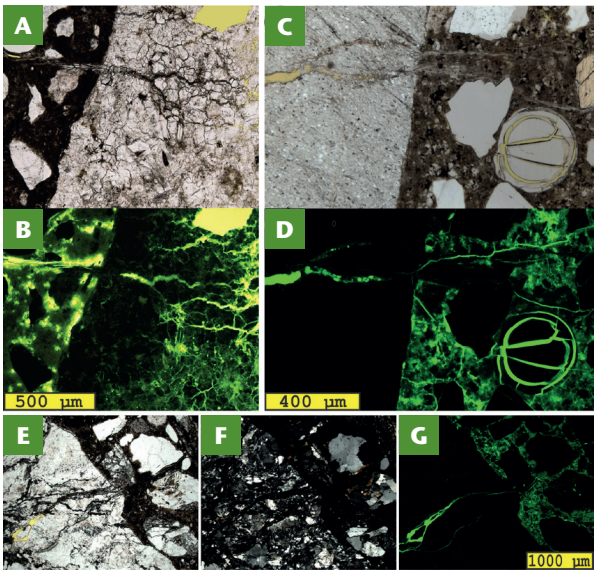

Figure 5 (**A**) Alkali-reactive aggregate particle of compacted sandstone in plane-polarized light with geliform ASR product squirting out into the embedding paste at left, and (**B**) the same view in fluorescent light. (**C**) Alkali-reactive particle of very fine-grained rhyolite and nearby air void–filled with desiccation-cracked ASR product, and (**D**) the same view in fluorescence. (**E**) Alkali-reactive cataclasite particle in plane-polarized light, and the same view in (**F**) cross-polarized light and (**G**) fluorescent light. Note that, in B, D, and G, the exuding gel completely plugs the crack it formed, implying active alkali reactivity.

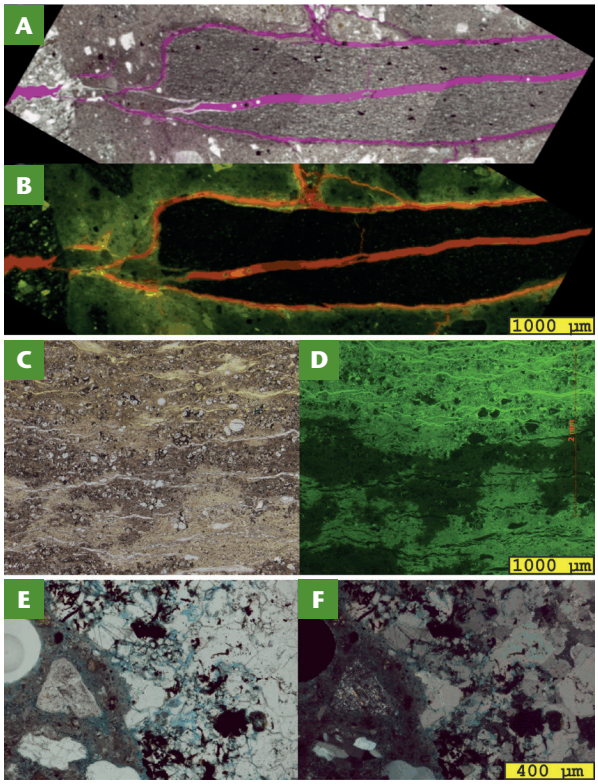

Figure 6 (**A**) Mosaic image of cracked alkali-reactive siltstone impregnated with pink epoxy, showing a typical crack that starts at the interior of the aggregate particles and then propagates into the cement paste, and (**B**) the same view in unfiltered fluorescence. (**C**) Deteriorated and partly corroded asbestos-reinforced concrete sewer pipe wall in plane-polarized light, and (**D**) the same view in fluorescence, revealing parts with enhanced porosity not identifiable in plain light, as well as surface-parallel delamination cracks. Note the unimpregnated fiber strands in the lower half, compared with the upper half. (**E**) Concrete affected by fire in which a blue epoxy (cf. Yanguas and Dravis 1985) highlights the open cracks in the porous limestone aggregate particle close to the contact with the cement paste. Note the unimpregnated air void on the left edge right under the panel marker, and (**F**) the same field of view in cross-polarized light.

microscopic crack patterns are not discernible without PFM on fluorescence-impregnated thin sections (Ingham 2011). FIGURES 6E and 6F present examples of concrete with fire damage. The limestone particle boundaries near the contact with the cement paste are open, made visible by the blue fluorescent dye, with no infilling products.

CONCLUSIONS AND OUTLOOK

Traditional thin section petrography is poorly suited for reliable assessment of quality and properties of (damaged) concrete because, without proper precautions, the soft and fragile material is easily destroyed during preparation. Vacuum impregnation with an epoxy of suitable quality improves the mechanical strength so much that preparation artefacts are minimized, provided the rigorous application of appropriate preparation procedures. Furthermore, addition of a blue-light fluorescent dye to the epoxy resin prior to impregnation provides visualization of the finest details of the internal porosity, crack patterns, mineral grain boundaries, and microtextures of the aggregates, as well as their spatial distributions. Polarization-fluorescence microscopy has become a routine method for concrete (damage) assessment in laboratories worldwide and is today an indispensable complementary analytical method when traditional engineering test methods are inconclusive. Compared with standard petrography, fluorescence-impregnation is far superior for visualizing the finest internal microstructural and textural/fabric features that remain hidden in plain light, with dramatically more contrast than blue epoxy (cf. Yanguas and Dravis 1985). Existing recent petrographic microscopes can almost always be retrofitted with standard filter kits. While a petrographic microscope with reflected light is recommended, satisfactory PFM can be achieved even with only transmitted light; expensive UV-illumination units are not needed. In summary, PFM represents a valuable extension of traditional petrography, requiring only minimal financial investment.

ACKNOWLEDGMENTS

This work was funded by the Portuguese Fundação para a Ciência e a Tecnologia (FCT) I.P./MCTES through national funds (PIDDAC) – UIDB/50019/2020, which are gratefully acknowledged. Contributions by OF and AM are supported by 'BASE3 – Basement weathering and fracturing on- and offshore Norway' under NFR grant 319849. The authors are grateful for comments from three anonymous referees who helped improve the manuscript's legibility. MATMB is grateful to Prof. Antonius (Ton) van Helvoort for helping retrieve a hardcopy of Romer and Dobrolubov (1974).

REFERENCES

Ashley GM (1973) Impregnation of fine-grained sediments with a polyester resin: a modification of Altemuller's method. Journal of Sedimentary Petrology 43: 298-301

ASTM (2022) Annual Book of ASTM Standards (04.02): Concrete and aggregates; (04.03): Road and paving materials; vehicle-pavement systems. American Society for Testing & Materials, West Conshohocken

Broekmans MATM (2009) Petrography as an essential complementary method in forensic assessment of concrete deterioration: two case studies. Materials Characterization 60: 644-655, doi: 10.1016/j.matchar.2008.12.017

Broekmans MATM (2012) Deleterious reactions of aggregate with alkalis in concrete. In: Broekmans MATM, Pöllmann H (eds) Applied Mineralogy of Cement and Concrete. Reviews in Mineralogy & Geochemistry 74: 279-364, doi: 10.1515/9781501508356-009

Broekmans MATM, Fernandes I (2015) Petrographic assessment of particulate materials: some statistical considerations. In: Çopuroğlu O (ed) Proceedings of the 15th Euroseminar on Microscopy Applied to Building Materials, Delft, pp 409-416

Camuti KS, McGuire PT (1999) Preparation of polished thin sections from poorly consolidated regolith and sediment materials. Sedimentary Geology 128: 171-178, doi: 10.1016/S0037-0738(99)00073-1

CAS Common Chemistry (2022) Solvent Yellow 43. https://commonchemistry.cas.org/detail?cas_rn=19125-99-6&search=19125-99-6 (accessed 06 December 2022)

CUR-Recommendation 102 (2008) Inspection and assessment of concrete structures in which ASR is suspected or has been confirmed. Official English translation. Centre for Civil Engineering Research & Codes, 31 pp

Elsen J, Lens N, Aarre T, Quenard D, Smolej V (1995) Determination of the w/c ratio of hardened cement paste and concrete samples on thin sections using automated image analysis techniques. Cement and Concrete Research 25: 827-834, doi: 10.1016/0008-8846(95)00073-L

Fernandes I, Broekmans MATM, Noronha F (2009) Petrography and geochemical analysis for the forensic assessment of concrete damage. In: Ritz K, Dawson L, Miller D (eds) Criminal and Environmental Soil Forensics. Springer, Dordrecht, pp 163-180, doi: 10.1007/978-1-4020-9204-6_11

Fernandes I, Ribeiro MA, Broekmans MATM, Sims I (2016) RILEM Recommended Test Method: Detection of potential alkali-reactivity – AAR-1.2. Petrographic Atlas: Characterisation of Aggregates Regarding Potential Reactivity to Alkalis. Springer, 193 pp

Gordon JE (1978) Structures, or why things don't fall down. Penguin Books, 395 pp

Hens HSLC (2012) Building Physics – Heat, Air and Moisture: Fundamentals and Engineering Methods with Examples and Exercises (Second Edition). Wiley-VCH Verlag, 315 pp

Ingham J (2011) Geomaterials Under the Microscope, A Colour Guide. Manson Publishing, 192 pp

Jägers E, Römich H, Müller-Weinitsche C (2000) Kapitel 6. Konservierungsmaterialien und Methoden. In: Wolff A (ed) Restaurierung und Konservierung historischer Glasmalereien. Verlag Phillipp von Zabern, Mainz, pp 129-166

Kubiëna WL (1938) Micropedology. Collegiate Press Inc., 243 pp

Leemann A, Katayama T, Fernandes I, Broekmans MATM (2016) Types of alkali–aggregate reactions and the products formed. Proceedings of the Institution of Civil Engineers – Construction Materials 169: 128-135, doi: 10.1680/jcoma.15.00059

Lindgård J and 6 coauthors (2010) The EU "PARTNER" project—European standard tests to prevent alkali reactions in aggregates: final results and recommendations. Cement and Concrete Research 40: 611-635, doi: 10.1016/j.cemconres.2009.09.004

Mather K (1953) Applications of light microscopy in concrete research. Symposium on Light Microscopy, American Society for Testing and Materials, Special Technical Publication 143, 51-70

Menéndez E and 11 coauthors (2022) RILEM TC 258-AAA round robin test: alkali release from aggregates and petrographic analysis. Critical review of the test method AAR-8. Materiales de Construcción 72: e279, doi: 10.3989/mc.2022.17021

Odler I (1998) 6 - Hydration, setting and hardening of Portland cement. In: Hewlett PC (ed) Lea's Chemistry of Cement and Concrete (Fourth Edition). Arnold Publishers, London, pp 241-297, doi: 10.1016/B978-075066256-7/50018-7

Poole AB, Sims I (2016) Concrete Petrography, A Handbook of Investigative Techniques (Second Edition). CRC Press, Taylor & Francis Group, 794 pp, doi: 10.1201/b18688

RILEM (2016) RILEM Recommended Test Method: AAR-1.1 – Detection of potential alkali-reactivity – part 1: petrographic examination method. In: Nixon PJ, Sims I (eds) RILEM recommendations for the prevention of damage by alkali-aggregate reactions in new concrete structures. Springer, Berlin. RILEM State-of-the-Art Report 17: 35-60

Romer B, Dobrolubov G (1974): Angewandte Mikroskopie bei der Baustoffprüfung – Beton, Mörtel, Zement, Kalk, Gips, Keramik. Leitz Mitteilungen für Wissenschaft und Technik, Wetzlar. Band (VI/4): 135-144.

Sims I, Poole AB (2017) Alkali–Aggregate Reaction in Concrete: A World-Review. CRC Press, 767 pp

The University of Edinburgh (2022) Sample preparation and sample requirements. The University of Edinburgh/SCO, School of Geosciences. https://www.ed.ac.uk/geosciences/about/facilities/all/ionprobe/technical/samples (accessed 05 December 2022)

Viola G and 5 coauthors (2016) Deconvoluting complex structural histories archived in brittle fault zones. Nature Communications 7: 13448, doi: 10.1038/ncomms13448

Wilk W, Dobrolubov G, Romer B (1974) Development in quality control of concrete during construction. Transportation Research Record 504: 1-26

Wong HS and 16 coauthors (2020) Microscopy techniques for determining water–cement (w/c) ratio in hardened concrete: a round-robin assessment. Materials and Structures 53: 25, doi: 10.1617/s11527-020-1458-2

Yanguas JE, Dravis JJ (1985) Blue fluorescent dye technique for recognition of microporosity in sedimentary rocks. Journal of Sedimentary Petrology 55: 600-602, doi: 10.2110/jsr.600 ■